NASA TECHNICAL NOTE

NASA TN D-6029

NASA TN D-6029

A DIRECT MEASUREMENT OF THE MOST PROBABLE PREFERRED ANGULAR VELOCITY OF TURBULENT STRUCTURES BY OPTICAL CORRELATION OF LASER SCHLIEREN SIGNALS

by B. H. Funk

George C. Marshall Space Flight Center
Marshall Space Flight Center, Ala. 35812

NATIONAL AERONAUTICS AND SPACE ADMINISTRATION • WASHINGTON, D. C. • OCTOBER 1970

1. Report No.	2. Government Accession No.	3. Recipient's Catalog No.
NASA TN D-6029		

4. Title and Subtitle

A Direct Measurement of the Most Probable Preferred Angular Velocity of Turbulent Structures by Optical Correlation of Laser Schlieren Signals

5. Report Date: October 1970

6. Performing Organization Code

7. Author(s)

B. H. Funk

8. Performing Organization Report No.

9. Performing Organization Name and Address

George C. Marshall Space Flight Center
Marshall Space Flight Center, Alabama 35812

10. Work Unit No.: M164

11. Contract or Grant No.

12. Sponsoring Agency Name and Address

13. Type of Report and Period Covered: Technical Note

14. Sponsoring Agency Code

15. Supplementary Notes

Prepared by Aero-Astrodynamics Laboratory, Science and Engineering Directorate
This report was first published August 26, 1969 as NASA TM X-53870.

16. Abstract

This report presents a method which potentially provides the means for separating the translational and rotational motion of turbulent structures. Simple two-dimensional models are used to relate the skewness of cross-correlograms computed from laser schlieren signals to the rotation of flow disturbances. The method, referred to herein as the method of "forced similarity," is discussed with respect to application to the turbulent free shear layer of an axisymmetric supersonic jet. Experimental results show that the shape of the cross-correlogram in the neighborhood of the "peak" is strongly influenced by rotational motion, and, therefore, it becomes necessary to account for the effect to determine the correct statistical properties of the turbulence.

17. Key Words (Suggested by Author(s))	18. Distribution Statement
	01, 12, 28

19. Security Classif. (of this report)	20. Security Classif. (of this page)	21. No. of Pages	22. Price*
Unclassified	Unclassified	32	$3.00

*For sale by the Clearinghouse for Federal Scientific and Technical Information
Springfield, Virginia 22151

TABLE OF CONTENTS

LIST OF ILLUSTRATIONS

DEFINITION OF SYMBOLS

Symbol	Definition
A	beam A, upstream beam
B	beam B, downstream beam
C	a constant ($C = 4\bar{I}_d/\pi D$)
D	diameter of laser beam; photodetector
$\bar{I}_d$	absolute time averaged current supplied to photodetector with knife-edge removed
i(t)	ac-electrical signal output of photodetector
$K(\xi, \psi_a, \psi_b, \psi_c)$	similarity function
$R(\xi,\tau)$	cross-correlation function or cross-correlogram of beam A
s	sensitivity of laser schlieren beam
T	integration time for computation of cross-correlation
t	time
$\langle U \rangle$	the most probable speed of disturbances averaged over the beam separation distance ξ
x, y, z	coordinates in direction of flow, perpendicular to flow direction (in horizontal plane), and perpendicular to flow direction (in vertical direction), respectively
a	Gladstone-Dale constant
$\underline{\Delta}$	beam deflection vector
ξ	beam separation distance
ρ	air density
τ	time delay of downstream signal
ϕ	angle of rotation of $\underline{\Delta}$ during transit time of disturbance from beam A to B
θ	angle measured from x-axis to beam deflection vector, $\underline{\Delta}$

DEFINITION OF SYMBOLS (Concluded)

Symbol	Definition
$\langle \underline{\omega}_p \rangle$	the most probable preferred angular velocity of the disturbances
$( )'$	fluctuating component
$\overline{( )}$	time average
$\underline{( )}$	vector
$\hat{( )}$	unit vector
$\langle \rangle$	expectation value, or most probable value
Subscripts	
x, y, z	component in direction of x, y, z-axis, respectively
a, b	beam A, B
c	refers to angle between beam B and the Z-axis
1, 2	case A, no rotation; case B, rotation
m	most probable; maximum

A DIRECT MEASUREMENT OF THE MOST PROBABLE PREFERRED ANGULAR VELOCITY OF TURBULENT STRUCTURES BY OPTICAL CORRELATION OF LASER SCHLIEREN SIGNALS

SUMMARY

This report presents a method that provides means for separating the translational and rotational motion of turbulent structures. Simple two-dimensional models are used to relate the skewness of cross-correlograms computed from laser schlieren signals to the rotation of flow disturbances. The method, referred to herein as the method of "forced similarity," is discussed with respect to application to the turbulent free shear layer of an axisymmetric supersonic jet. Experimental results show that the shape of the cross-correlogram in the neighborhood of the "peak" is strongly influenced by rotational motion, and, therefore, it becomes necessary to account for the effect to determine the correct statistical properties of the turbulence.

INTRODUCTION

This report contains the author's preliminary thoughts on the possibility of making direct measurements of the most probable preferred angular velocity at "localized" regions within turbulent flows by optical correlations of laser schlieren signals [1]. Although some experimental results are presented which satisfy certain necessary conditions required of the proposed theory, sufficient data verifying the theory do not exist. However, plans have been made to obtain these data in Marshall Space Flight Center's Cold Flow Thermal and Acoustic Jet Facility.

During the feasibility test presented in Reference 1, there were unexplained variations in the shape of the cross-correlograms computed from laser schlieren signals retrieved from the supersonic turbulent boundary layer on a thin plate. In April 1968, near the conclusion of this test, the connection between the skewness of the cross-correlograms and the angular rotation of the disturbances was considered.

Preliminary experimental results eventually led to a method for separating rotational and translational contributions to the computed cross-correlograms. This method is referred to herein as the method of "forced similarity." The "forced similarity" condition provides the means for direct measurement of the most probable preferred[1] angular velocity of the turbulent structures[2] at localized

---

1. The word "preferred" is used since the statistical process does not yield the angular velocity components based upon statistical averages of absolute values.

2. Throughout this report reference is made to "turbulent structures" and "disturbances" to distinguish between the motion of the density gradient and the motion of fluid particles which represent an "eddy" at a particular instant. The laser schlieren signals are produced by the fluctuating density gradient component perpendicular to the path of the beam [2].

regions inside turbulent flows. The potential extension of the method to yield the probability distribution of the angular velocity and measurements of vorticity are very interesting, and may result as a natural consequence of the development of the laser schlieren system.

THE LASER SCHLIEREN OPTICAL REMOTE SENSING SYSTEM

For simplicity, consider the model of a laser schlieren optical remote sensing system [1] shown in Figure 1 where two laser beams of light are directed through the test section of a wind tunnel. The parallel beams are perpendicular to the flow and are separated by a distance ξ. The plane formed by the beams is such that flow disturbances passing through the upstream beam (beam A) at time t, also pass through the downstream beam (beam B) at a later time $t + \tau$. A knife-edge is positioned perpendicular to each of the beams such that 50 percent of the light is prevented from reaching the respective photodetectors when the beams are undisturbed.

Reference 2 shows that a disturbance characterized by a local gradient of the index of refraction will deflect each of these beams as it passes through them. Each deflection is proportional to the component of the gradient that is perpendicular to the path of the beam. When a deflection occurs, the amount of light on the photodetector changes. The photodetector converts this change into an ac signal. Therefore, the output signal of the photodetector is related to the beam deflection which is caused by a local gradient characterizing a particular flow disturbance passing through the laser beam.

Because the refractive index of air is proportional to the density (to a good approximation), the output signal of the photodetector is proportional to the change in the component of the density gradient which is perpendicular to the beam and to the knife-edge.

$$i(t) \doteq a \int_{-\ell}^{\ell} s \frac{\partial \rho}{\partial x} \, dy \qquad . \tag{1}$$

In equation (1), s is the sensitivity of the beam, a is the Gladstone-Dale constant [2], and $i(t)$ is the output signal of the photodetector. Also, the knife-edge was assumed to be perpendicular to the x-direction as shown in Figure 2.

Figure 2, a view taken along the centerline of the laser beam (either beam A or B) from laser toward detector, shows the knife-edge, the eye of the photodiode, and the laser beam cross section. The beam is shown in the undisturbed position and in a deflected position described by the beam deflection vector, $\underline{\Delta}$.

In the following, let $\Delta(t)$ and $\theta(t)$ represent the magnitude and direction of $\underline{\Delta}(t)$, respectively. Further, assume that the eye of the photodiode has a large area of constant sensitivity compared to the cross-sectional area of the laser beam, and that no laser light falls outside of this area of constant sensitivity. If the intensity across the laser beam is assumed to be constant over the beam cross section and that the knife-edge is straight, the relationship between the time histories of the beam deflection vector and the photodetector ac output is simplified considerably.

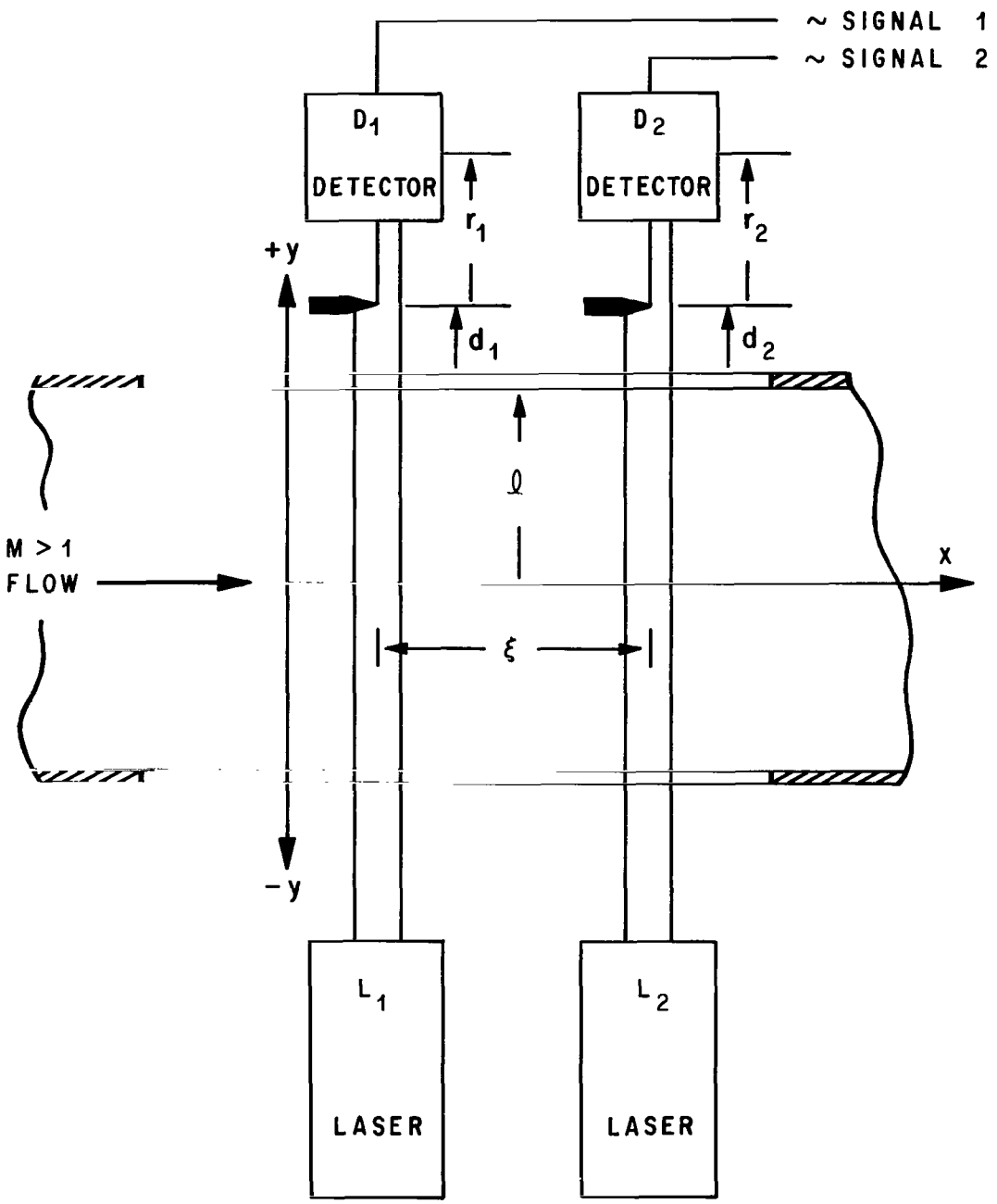

Figure 1. A schematic of a laser schlieren system using parallel beams.

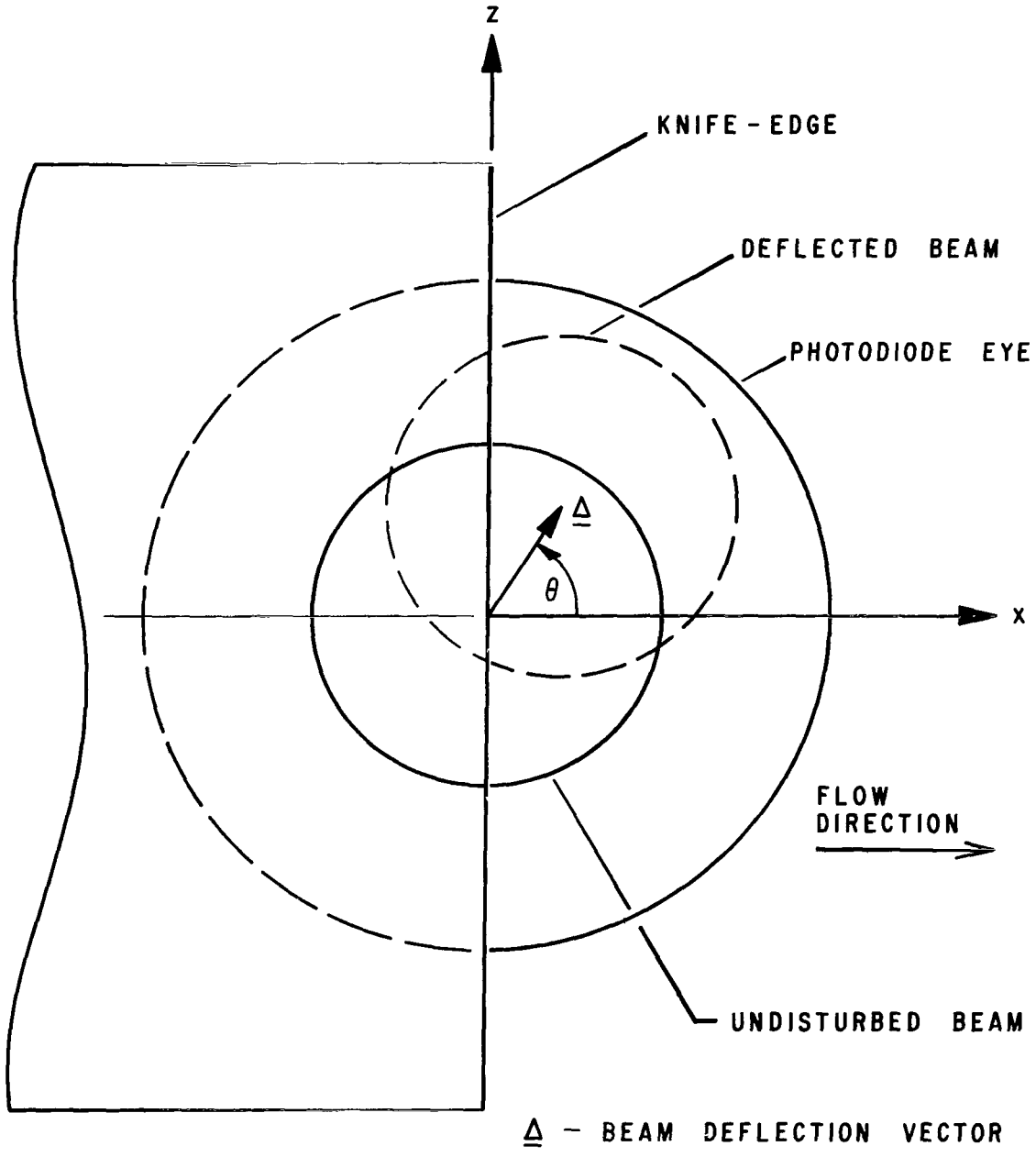

Figure 2. A schematic of a cross section taken across one beam of a laser schlieren system.

Because the area of sensitivity of the eye of the photodiode monitoring the fluctuating laser light is constant, the component of the beam deflection vector which is parallel to the knife-edge does not contribute to the output signal of the photodetector. The component of $\underline{\Delta}$ which is perpendicular to the knife-edge will determine the amount of change in light reaching the photodiode. If the beam deflection is small compared to the diameter of the laser beam, the output signal, i(t), can be expressed conveniently as a function of the component $\underline{\Delta}$ which is perpendicular to the knife-edge:

$$i(t) = \left(\frac{4\bar{I}_d}{\pi D} \right) \Delta_x(t) \quad , \tag{2}$$

where the first group of terms in parentheses on the right-hand side of equation (2) is the change in the output signal per unit change in Δ_x and is assumed to be a constant, C.

$$i(t) = C \cdot \Delta_x(t) \quad . \tag{3}$$

For this case, the photodetector output is a linear function of the component of $\underline{\Delta}$ which is normal to the knife-edge. This result is not unrealistic and can be approximated very well in practice.

Since

$$\Delta_x(t) = \Delta(t) \cdot \cos\theta(t) \quad , \tag{4}$$

equation (3) can be expressed as

$$i(i) = C \cdot \Delta(t) \cdot \cos\theta(t) \quad . \tag{5}$$

Thus, we see from equation (5) that i(t) is a function of the direction as well as the magnitude of the beam deflection vector.

For the laser schlieren system shown in Figure 1, the signals from the photodetectors monitoring the respective beams are

$$i_a(t) = C_a \cdot \Delta_a(t) \cdot \cos\theta_a(t) \tag{6}$$

and

$$i_b(t) = C_b \cdot \Delta_b(t) \cdot \cos\theta_b(t) \quad . \tag{7}$$

Assume that the turbulence is two-dimensional; i.e., the time-averaged statistical properties do not vary along the beams. Although this assumption will restrict the analysis, it provides a better model for the purpose of describing the fundamental concept, the prime purpose here. It will soon become evident that relaxing this assumption will not change the fundamental relationship between the shape of the correlograms and the angular velocity of the density gradient vector component which is normal to the respective beams.

The cross-correlation of the signals $i_a(t)$ with $i_b(t + \tau)$ is given by [3]

$$R(\xi,\tau) = \lim_{T\to\infty} \frac{1}{T} \int_0^T i_a(t) \cdot i_b(t + \tau)\, dt \quad . \tag{8}$$

Substitute equations (6) and (7) into (8) and assume that the integration time, T, is large enough so that

$$R(\xi,\tau) = \frac{C_a C_b}{T} \int_0^T \Delta_a(t) \cdot \Delta_b(t + \tau) \cdot \cos\theta_a(t) \cdot \cos\theta_b(t + \tau)\, dt \tag{9}$$

Figure 3 shows the knife-edge orientation for the cross-correlation of equation (9). This figure also shows the beam deflection vector of beam A at time t when a particular disturbance is passing through the beam, and the $\underline{\Delta}$ of beam B when the same disturbance is passing through beam B at a later time $t + \tau$. When this disturbance passes through beam A, the beam is deflected in a direction θ_a, and by a magnitude of Δ_a. This magnitude of the deflection vector is determined by the magnitude of the density gradient component normal to the beam characterizing the disturbance. The direction of the deflection is caused by the particular orientation of the same density gradient component. If the realistic assumption is made that the disturbance rotates as it travels downstream, its orientation will not necessarily be the same when it passes through beam B as it was when it passed through beam A. This is represented in Figure 3 where the beam deflection vector caused by a particular disturbance has rotated during its transit from beam A to beam B. It follows that

$$\left| \underline{\Delta}_a(t) \times \underline{\Delta}_b(t + \tau) \right| = \Delta_a(t) \cdot \Delta_b(t + \tau) \cdot \sin\phi(t + \tau) \quad . \tag{10}$$

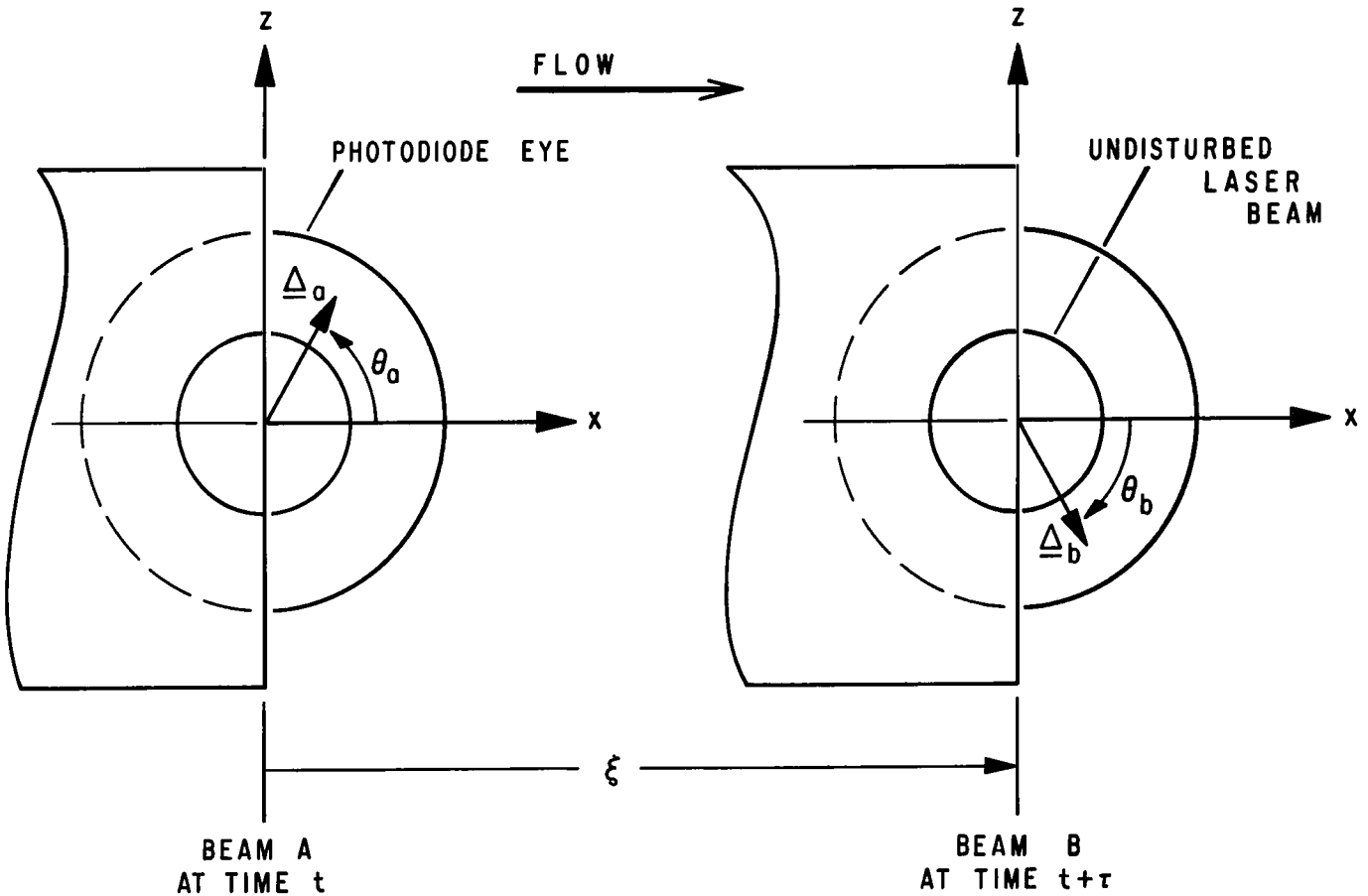

Figure 3. A schematic of a view taken along laser beams of the laser schlieren system shown in Figure 1.

This equation defines the angle ϕ through which the disturbance rotated during transit from beam A to B. Thus,

$$\phi(t + \tau) = \theta_a(t) - \theta_b(t + \tau) \tag{11}$$

Solving equation (11) for $\theta_b(t + \tau)$ and substituting into equation (9) gives

$$R(\xi,\tau) = \frac{C_a C_b}{T} \int_0^T \Delta_a(t) \cdot \Delta_b(t + \tau) \cdot \cos \theta_a(t) \cdot \cos [\theta_a(t) - \phi(t + \tau)] \, dt \quad . \tag{12}$$

To examine the effect which this angular rotation has upon the cross-correlation function $R(\xi,\tau)$, consider a simplified two-dimensional flow model where it is assumed that the disturbances are random and produce statistically stationary signals. The cross-correlation function [equation (12)] will be studied for two cases: (a) where the disturbances do not rotate and (b) where each disturbance rotates through the same angle, ϕ, during transit from beam A to beam B. Case (a) will be discussed first.

Figure 4 shows four knife-edge arrangements where the view is taken along the laser beams similar to that of Figure 3. The differences between these four figures is the orientation of the downstream knife-edge. If we assume that the disturbances do not rotate, then

$$\phi(t + \tau) = 0 \quad , \tag{13}$$

and from equation (11),

$$\theta_b(t + \tau) = \theta_a(t) \quad . \tag{14}$$

The signal from beam A will be

$$i_a(t) = C_a \cdot \Delta_a(t) \cdot \cos \theta_a(t) \tag{15}$$

and is the same for all four knife-edge arrangements.

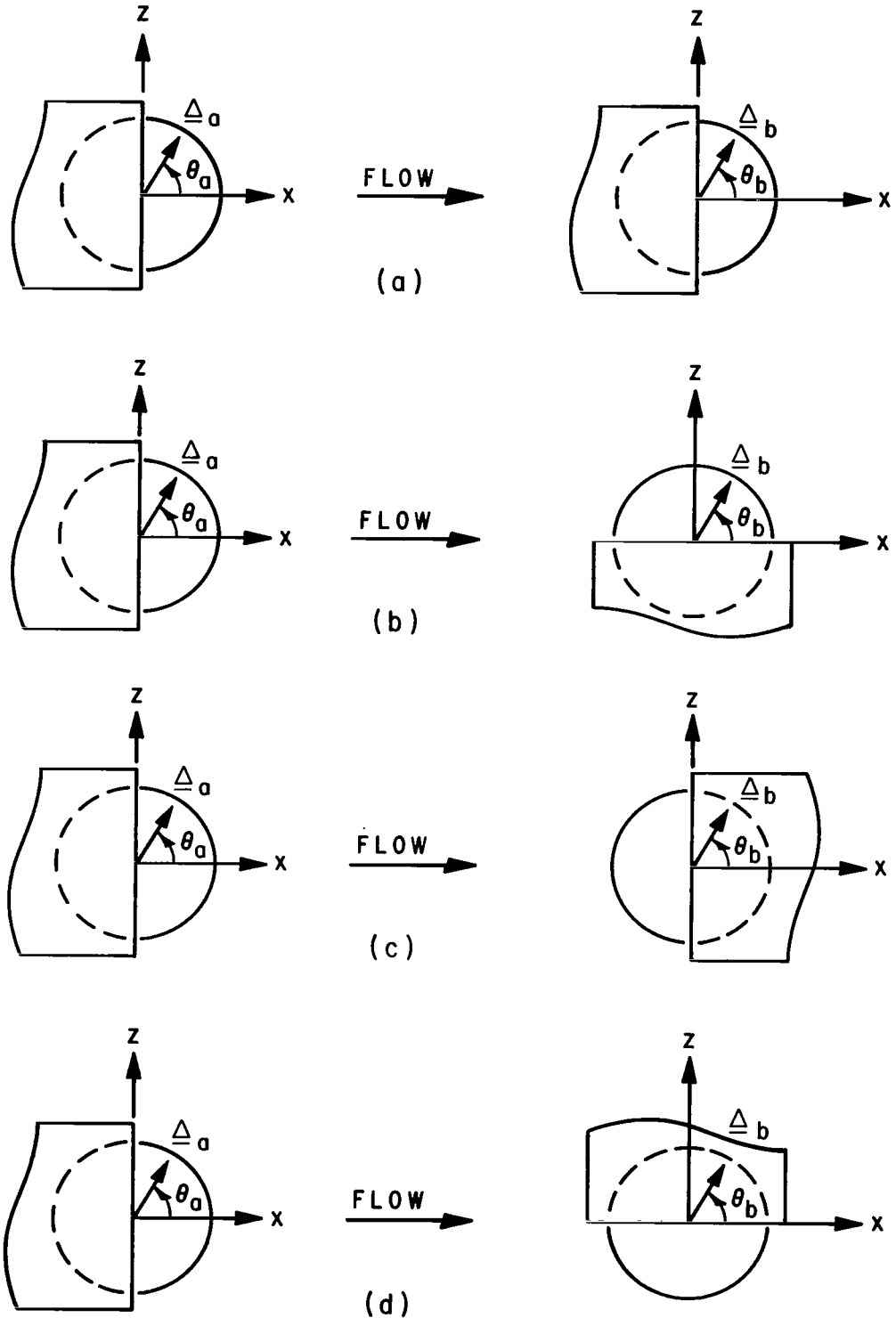

Figure 4. A schematic of four knife-edge arrangements of the laser schlieren system shown in Figure 1.

The signals from beam B for Figure 4a through 4d are

$$i_{b1}(t+\tau) = C_b \cdot \Delta_b(t+\tau) \cdot \cos\theta_b(t+\tau) \quad , \tag{16}$$

$$i_{b2}(t+\tau) = C_b \cdot \Delta_b(t+\tau) \cdot \sin\theta_b(t+\tau) \quad , \tag{17}$$

$$i_{b3}(t+\tau) = -C_b \cdot \Delta_b(t+\tau) \cdot \cos\theta_b(t+\tau) \quad , \tag{18}$$

$$i_{b4}(t+\tau) = -C_b \cdot \Delta_b(t+\tau) \cdot \sin\theta_b(t+\tau) \quad , \tag{19}$$

respectively.

When we substitute equation (14) into equations (16), (17), (18), and (19), the cross-correlation functions for the respective knife-edge arrangements become

$$R_1(\xi,\tau) = \left(\frac{C_a C_b}{T}\right) \int_0^T \Delta_a(t) \cdot \Delta_b(t+\tau) \cdot \cos\theta_a(t) \cdot \cos\theta_a(t)\, dt \quad , \tag{20}$$

$$R_2(\xi,\tau) = \left(\frac{C_a C_b}{T}\right) \int_0^T \Delta_a(t) \cdot \Delta_b(t+\tau) \cdot \cos\theta_a(t) \cdot \sin\theta_a(t)\, dt \quad , \tag{21}$$

$$R_3(\xi,\tau) = -\left(\frac{C_a C_b}{T}\right) \int_0^T \Delta_a(t) \cdot \Delta_b(t+\tau) \cdot \cos\theta_a(t) \cdot \cos\theta_a(t)\, dt \quad , \tag{22}$$

$$R_4(\xi,\tau) = -\left(\frac{C_a C_b}{T}\right) \int_0^T \Delta_a(t) \cdot \Delta_b(t+\tau) \cos\theta_a(t) \cdot \sin\theta_a(t)\, dt \quad . \tag{23}$$

The cross-correlograms for these arrangements are shown in Figure 5a, 5b, 5c, and 5d, respectively. An example of a cross-correlogram, represented by equation (20), would be similar to that shown in Figure 6a. A cross-correlogram similar to that represented by equation (22) is shown in Figure 6b.

For case B, it is assumed that each disturbance rotates through the same angle ϕ during transit from beam A to B; then,

$$\phi(t+\tau) = \phi \tag{24}$$

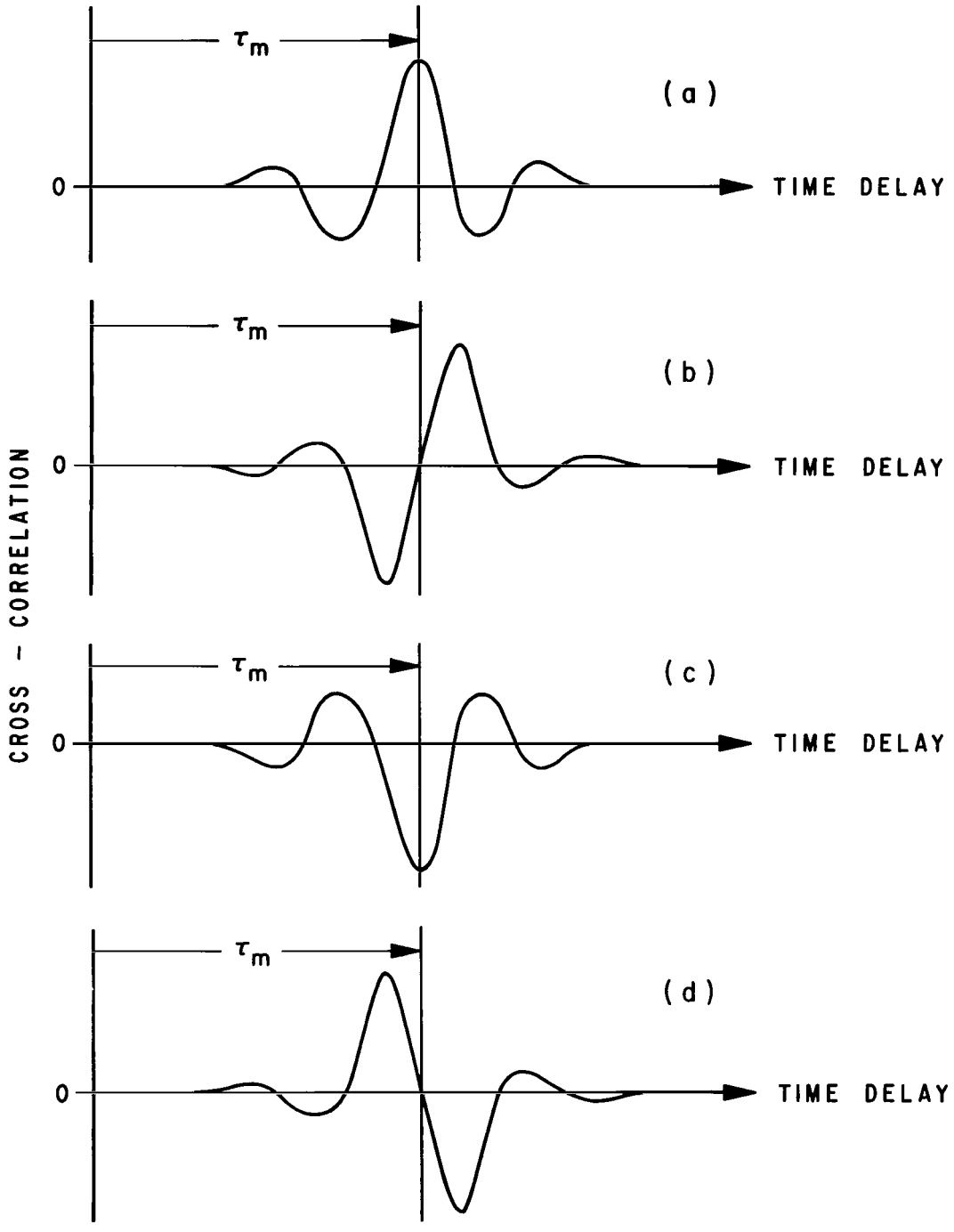

Figure 5. Schematic of cross-correlograms corresponding to the knife-edge arrangements in Figure 4, respectively.

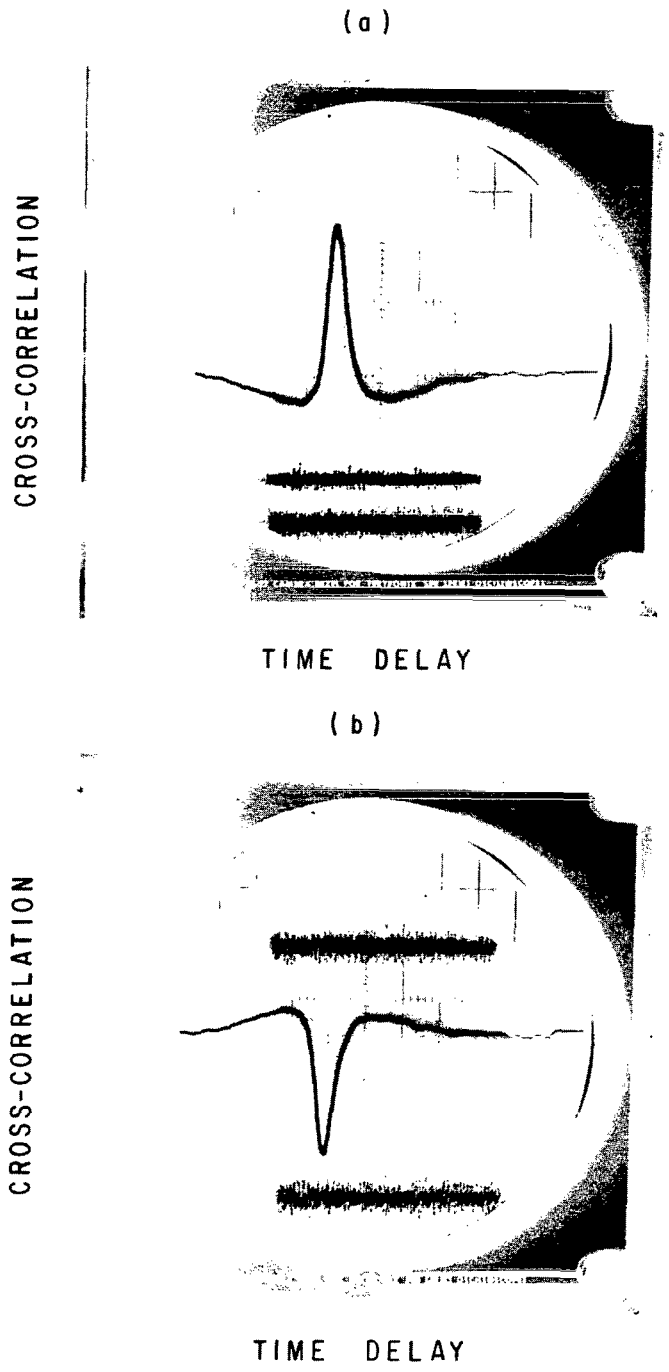

Figure 6. (a) Typical cross-correlogram for knife-edge arrangement of Figure 4(a) [equation (20)], (b) Typical cross-correlogram for knife-edge arrangement of Figure 4(c) [equation (22)].

Expanding equation (12) and making the substitution from equation (24),

$$R(\xi,\tau) = \left(\frac{C_a C_b}{T}\right) \int_0^T \Delta_a(t) \cdot \Delta_b(t+\tau) \cdot \cos^2\theta_a(t) \cdot \cos\phi \, dt$$

$$+ \left(\frac{C_a C_b}{T}\right) \int_0^T \Delta_a(t) \cdot \Delta_b(t+\tau) \cdot \cos\theta_a(t) \cdot \sin\theta_a(t) \cdot \sin\phi \, dt \qquad (25)$$

Since ϕ is not a function of time, $\cos\phi$ and $\sin\phi$ can be taken outside of the integrals on the right-hand side of equation (25), respectively.

$$R(\xi,\tau) = [\cos\phi] \left(\frac{C_a C_b}{T}\right) \int_0^T \Delta_a(t) \cdot \Delta_b(t+\tau) \cdot \cos^2\theta_a(t) \, dt$$

$$+ [\sin\phi] \left(\frac{C_a C_b}{T}\right) \int_0^T \Delta_a(t) \cdot \Delta_b(t+\tau) \cdot \cos\theta_a(t) \cdot \sin\theta_a(t) \, dt \qquad (26)$$

In equation (26), the integrals represent the cross-correlations derived for case A. Substitution of equations (20) and (21) into (26) yields

$$R(\xi,\tau) = [\cos\phi] \, R_1(\xi,\tau) + [\sin\phi] \, R_2(\xi,\tau) \qquad (27)$$

Equation (27) relates the cross-correlogram of case B to those of case A. Equation (27) shows that

$$R(\xi,\tau) = R_1(\xi,\tau) \quad , \qquad \text{for } \phi = 0 \qquad (28)$$

$$R(\xi,\tau) = R_2(\xi,\tau) \quad , \qquad \text{for } \phi = \pi/2 \qquad (29)$$

$$R(\xi,\tau) = -R_1(\xi,\tau) \quad , \qquad \text{for } \phi = \pi \qquad (30)$$

$$R(\xi,\tau) = -R_2(\xi,\tau) \quad , \qquad \text{for } \phi(3/2)\,\pi \qquad (31)$$

as should be expected.

In equation (27), the unknown quantity is the angle, ϕ. A direct measurement of ϕ for the idealized model in case B can be made by combining case A with case B. This procedure is referred to here as the method of "forced similarity" and is as follows:

(1) Compute the cross-correlogram $R(\xi,\tau)$ for zero beam separation with the knife-edges as shown in Figure 2 ($\xi = 0$). Since $\phi = 0$ for $\xi = 0$,

$$R(0,\tau) = R_1(0,\tau) \quad . \tag{32}$$

(2) Separate the two beams by moving beam B downstream a known distance ξ from beam A. The position and knife-edge angle, ψ_a, of beam A are not changed ($\psi_a = 0$).

(3) Rotate the downstream knife-edge, B, to the angle, ψ_{bm}, which produces the same "shape" of the cross-correlogram as was computed for zero beam separation. For this simplified flow model, the angle, ψ_{bm}, corresponding to the maximum "degree of similarity" between the cross-correlograms is equal to the angle, ϕ, through which the disturbances rotate during transit from beam A to beam B. The "forced similarity" condition is

$$R(\xi,\tau - \tau_m, \psi_b) = K(\xi,\tau,\psi_b) \cdot R(0,\tau) \tag{33}$$

where $K(\xi,\tau,\psi_b)$ is "optimum" when $\psi_b = \psi_{bm}$ for a particular ξ.

(4) The most probable transit time, τ_m, of the disturbances is determined by the time delay on the cross-correlogram for separated beams corresponding to the similar position at zero time delay on the cross-correlogram for zero beam separation.

(5) The most probable speed of the disturbances is

$$\langle U \rangle \doteq \xi \tau_m \tag{34}$$

(6) The most probable angular velocity is

$$\langle \underline{\omega}_p \rangle \doteq \phi \tau_m = \psi_{bm} \tau_m \quad . \tag{35}$$

These models have been used to relate the experimentally observed skewness of cross-correlograms, computed from laser schlieren signals, to the rotation of the turbulent structures.

PRACTICAL APPLICATION OF THE METHOD OF FORCED SIMILARITY

In the previous section, a method of "forced similarity" was introduced which provides the means for measuring the most probable preferred angular velocity of the simplified two-dimensional disturbances. As a consequence of the proposed relation between the skewness of the cross-correlogram and the rotational motion of the disturbances, the "forced similarity" condition, equation (33), must be imposed to determine the most probable transit time, τ_m, as well as all other statistical properties which are computed from the shape of the cross-correlogram in the neighborhood of τ_m. Imposing this condition analytically involves normalization of the cross-correlogram and optimization of the similarity function, $K(\xi,\tau,\psi_b)$. These details will not be discussed here. Rather, we will proceed to the practical application.

Figure 7 shows a schematic of the free jet shear layer of a supersonic axisymmetric air jet. Two laser beams are directed through the flow perpendicular to one another and in such a manner that the plane formed by the beams is perpendicular to the centerline of the jet. The horizontal beam (beam A) passes through the center of the jet. The vertical beam (beam B) passes through the shear layer and intersects the horizontal beam as shown in Figure 7.

In Reference 4, it is theoretically shown that the statistical cross-correlation of the signals from two such beams should result in a cross-correlogram representative of the components of the signals which are caused by disturbances passing through the localized region about the beam intersection; i.e., flow disturbances passing through the beams that are not common to both beams do not contribute significantly to the cross-correlogram (the integration time being sufficiently long). In Reference 1, the experimental verification of this "cross-beam" concept was successfully achieved in a supersonic (M = 2.0) turbulent wake of a thin flat plate.

Referring again to the axisymmetric jet, the "forced similarity" condition may be satisfied for retrieving all three components of the most probable preferred angular velocity, $\langle \underline{\omega}_p \rangle$, of the disturbances passing through a localized region of the shear layer. It may be assumed that the mean statistical properties of the turbulence are also axisymmetric, and thereby eliminate one component of $\langle \underline{\omega}_p \rangle$; however, this is not necessary and will not be done.

The experimental procedure is as follows:

(1) The beams are directed through the turbulence as shown in Figure 7 with zero beam intersection ($\xi = 0$). The knife-edges are positioned as shown ($\psi_a = 0$ and $\psi_b = 0$).

(2) The cross-correlogram $R(0,\tau)$ is computed.

(3) The vertical beam (beam B) is moved downstream a distance ξ as shown in Figure 8, and the cross-correlogram $R(\xi,\tau)$ is computed which satisfies the "forced similarity" condition

$$R(\xi,\tau - \tau_m, \psi_{am}, \psi_{bm}) = K(\xi, \tau, \psi_{am}, \psi_{bm}) \cdot R(0,\tau) \qquad (36)$$

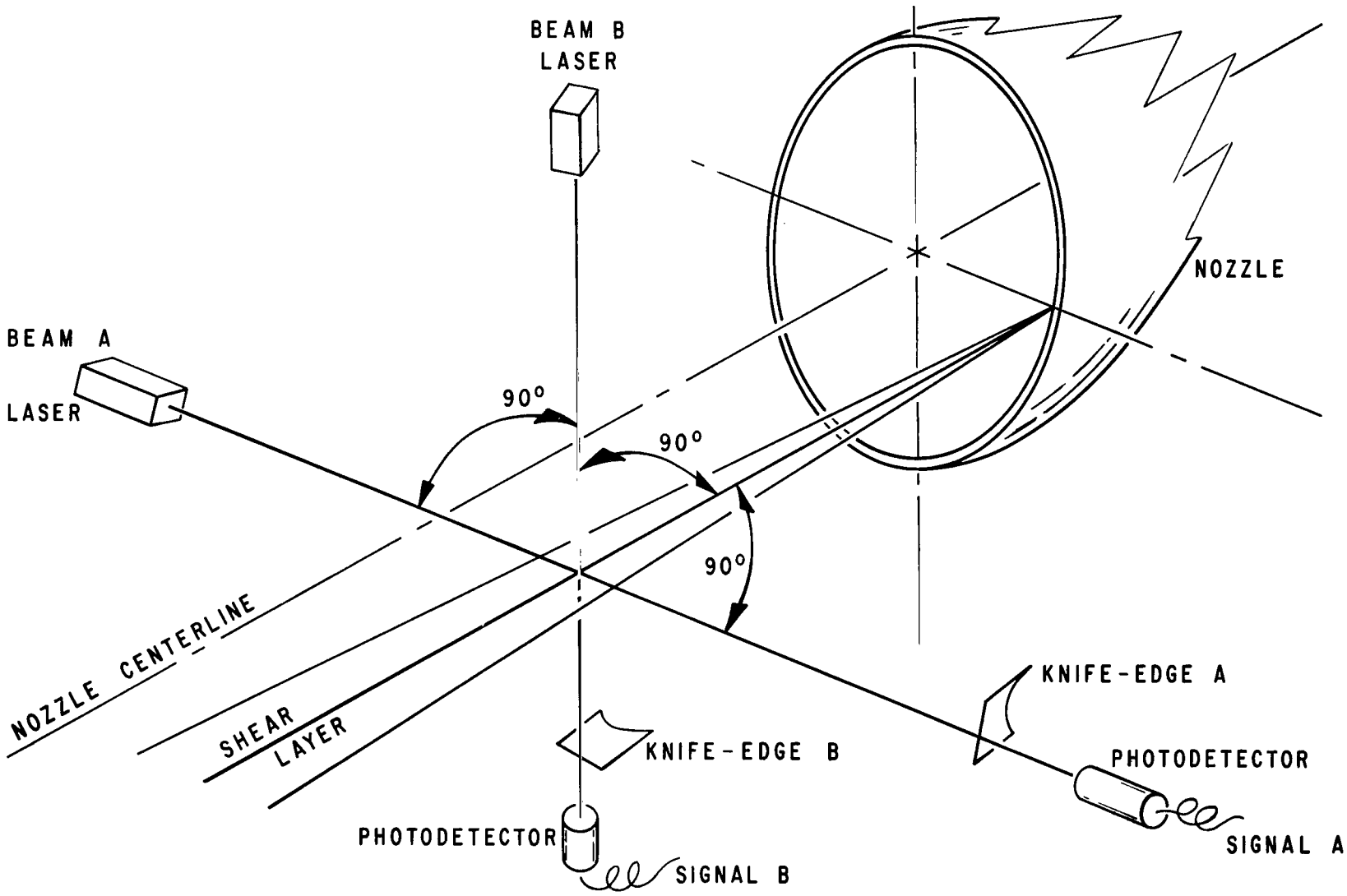

Figure 7. Cross-beam arrangement for axisymmetric jet.

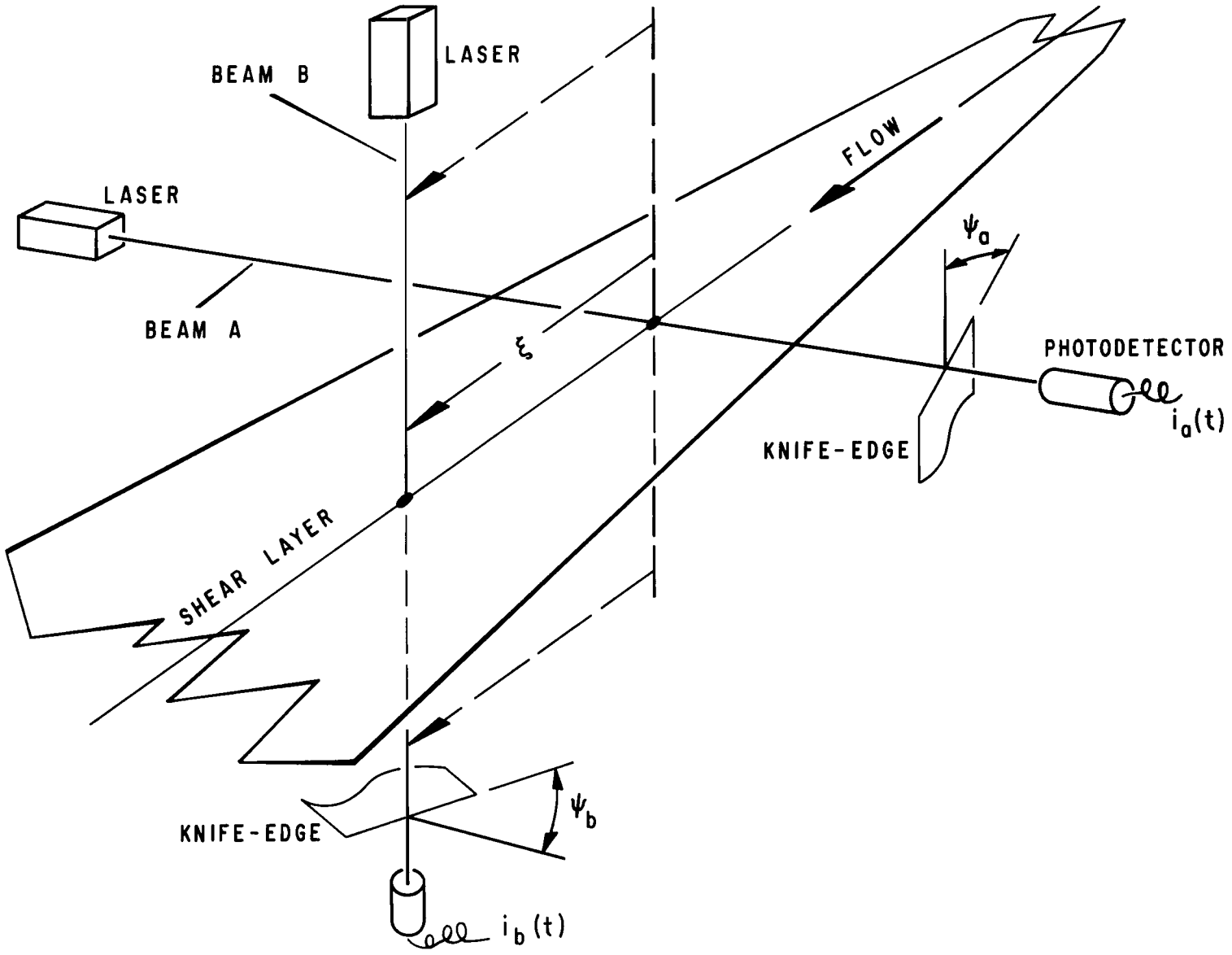

Figure 8. Schematic of space-time correlation satisfying the "forced similarity" condition.

for axisymmetric flows. $K(\xi, \tau, \psi_{am}, \psi_{bm})$ is determined to be the "weakness" function necessary to satisfy equation (36) in the neighborhood of τ_m. Experimentally, this involves rotation of both of the knife-edges. When this step is completed, the condition should be satisfied for this particular flow.

(4) If necessary, the next step would be to rotate the downstream beam in the plane perpendicular to the centerline of the jet. This is done in increments and step (3) is repeated for each increment until all three angles ψ_a, ψ_b, and ψ_c have been determined which satisfy the three-dimensional similarity condition

$$R(\xi, \tau - \tau_m, \psi_{am}, \psi_{bm}, \psi_{cm}) = K(\xi, \tau, \psi_{am}, \psi_{bm}, \psi_{cm}) \cdot R(0,\tau) \tag{37}$$

where ψ_c is the angle of rotation of the vertical beam.

(5) The most probable transit time of the disturbances is determined by evaluating the similarity condition (37) for $\tau = 0$:

$$R(\xi, 0 - \tau_m, \psi_{am}, \psi_{bm}, \psi_{cm}) = \frac{R(0,0)}{K(\xi, 0, \psi_{am}, \psi_{bm}, \psi_{cm})} \tag{38}$$

Thus, τ_m is equal to the time delay on the cross-correlogram $R(\xi, \tau, \psi_{am}, \psi_{bm}, \psi_{cm})$ corresponding to the similar position at zero time delay on the cross-correlogram for zero beam separation.

(6) The components of the most probable preferred angular velocity are

$$\langle\omega_x\rangle \doteq \frac{\psi_{cm}}{\tau_m} \tag{39}$$

$$\langle\omega_y\rangle = \frac{-\psi_{am}}{\tau_m} \tag{40}$$

$$\langle\omega_z\rangle = \frac{\psi_{bm}}{\tau_m} \tag{41}$$

and the most probable vector is

$$\langle\underline{\omega}_p\rangle = \hat{i}\langle\omega_x\rangle + \hat{j}\langle\omega_y\rangle + \hat{k}\langle\omega_z\rangle \tag{42}$$

(7) The most probable speed of transit is

$$\langle U \rangle = \frac{\xi}{\tau_m} \quad . \tag{43}$$

Figures 9 and 10 show the first successful cross-beam measurements in the supersonic free shear layer of an axisymmetric jet. The nozzle exit Mach number was 2.5, and the expansion was optimum.

Figures 9a and 9b show the positive and negative time delay ranges of the cross-correlogram. The beam geometry is shown in Figure 7 ($\xi = 0$). It can be seen that the correlogram is not symmetric about the origin ($\tau = 0$), but that there is a dominant peak at ($\tau = 0$). This cross-correlogram corresponds to $R(0,\tau)$ in equation (36).

Figure 10 shows the cross-correlogram for a beam separation of 1 inch ($\xi = 1''$) with the knife-edges in the same positions as in Figure 9 ($\psi_a = 0$, $\psi_b = 0$). The fact that there is a considerable difference in the shapes of these correlograms satisfies one necessary condition required by the theory of "forced similarity."

Figure 11 shows four cross-correlations computed from signals retrieved with a laser schlieren system using parallel beams as previously described. The data[3] were retrieved from the supersonic (M = 2.0) turbulent boundary layer on the thin plate shown in Figure 12. The beams were separated by approximately 1.5 inches in the direction of flow and were approximately 1/8 inch above the surface of the plate. These cross-correlograms were computed with the downstream knife-edge orientations shown and were the first experimental attempt to relate the shape of the correlogram, in the neighborhood of the most probable transit time, τ_m, to the orientation of the knife-edges relative to the flow and to each other.

These data show that the relative orientation of the knife-edges to each other does indeed influence the shape of the cross-correlogram. Therefore, it is reasonable to consider that the cross-correlogram is influenced by a change in the relative orientation of the disturbances to the knife-edges as they translate from one to the other.

CONCLUSIONS

Based upon the theoretical and experimental results which have been presented, the following conclusions are:

---

3. These measurements were made in MSFC's Bisonic Wind Tunnel on June 3, 1969 [1].

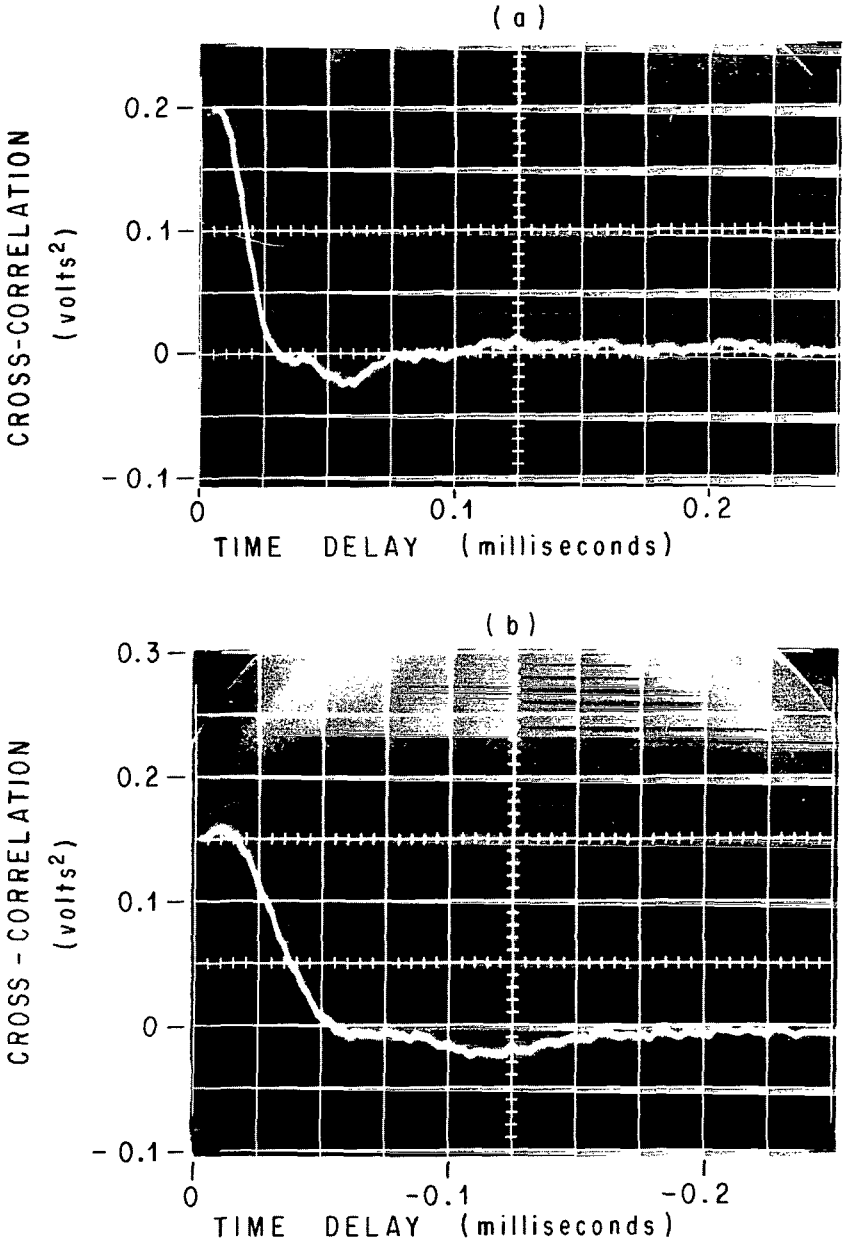

Figure 9. Cross-correlogram computed from laser schlieren signals retrieved from free shear layer of axisymmetric jet (M_e = 2.5), (a) positive time delay range, (b) negative time delay range.

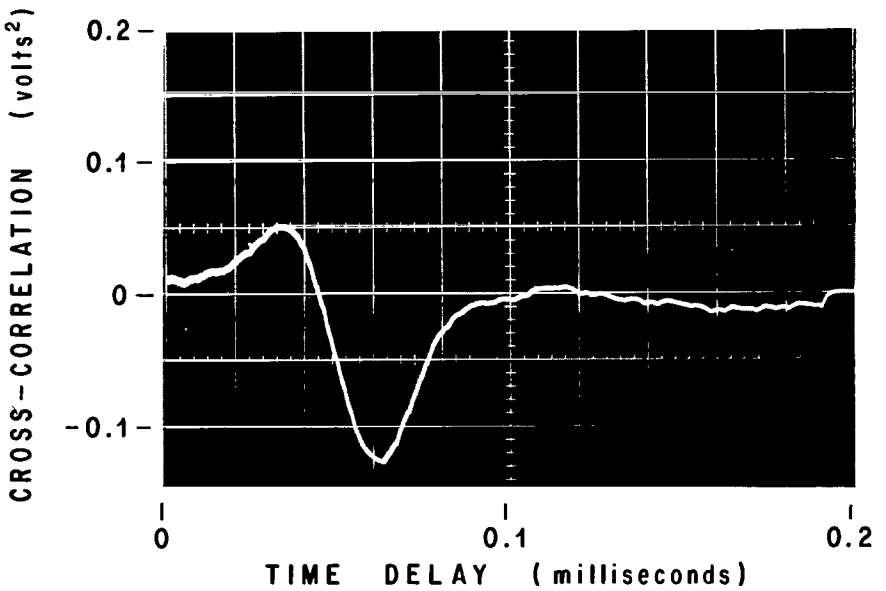

Figure 10. Cross-correlogram computed for same case as that of Figure 9 except beams are separated by 1.0 inch as shown in Figure 8 ($\psi_a = 0, \psi_b = 0$).

(1) The relative orientation of the knife-edges to each other controls the shape of the cross-correlogram in the neighborhood of the time delay, τ_m, corresponding to the most probable transit time of disturbances between the laser beams.

(2) The method of "forced similarity" introduced here provides the means for separating the translational and rotational contributions to the shape of the cross-correlogram. However, more experimental results are needed for verification.

(3) The "forced similarity" condition is based upon the assumption that the shape of the cross-correlogram computed with beams separated is "similar" to that computed with zero beam separation when the contribution caused by rotation has been eliminated (the effect of decay accepted).

(4) Because of the rotational influences, significant error can result in the flow properties which are computed from the shape of the cross-correlogram unless the influence caused by rotation is considered.

(5) The condition of "forced similarity" may be applied by rotation of either or both beams about the axes of a reference coordinate system in combination with rotation of the knife-edges. The particular combination used is primarily dependent upon the flow.

George C. Marshall Space Flight Center
National Aeronautics and Space Administration
Marshall Space Flight Center, Alabama 35812, June 29, 1970
976-30-20-00-75

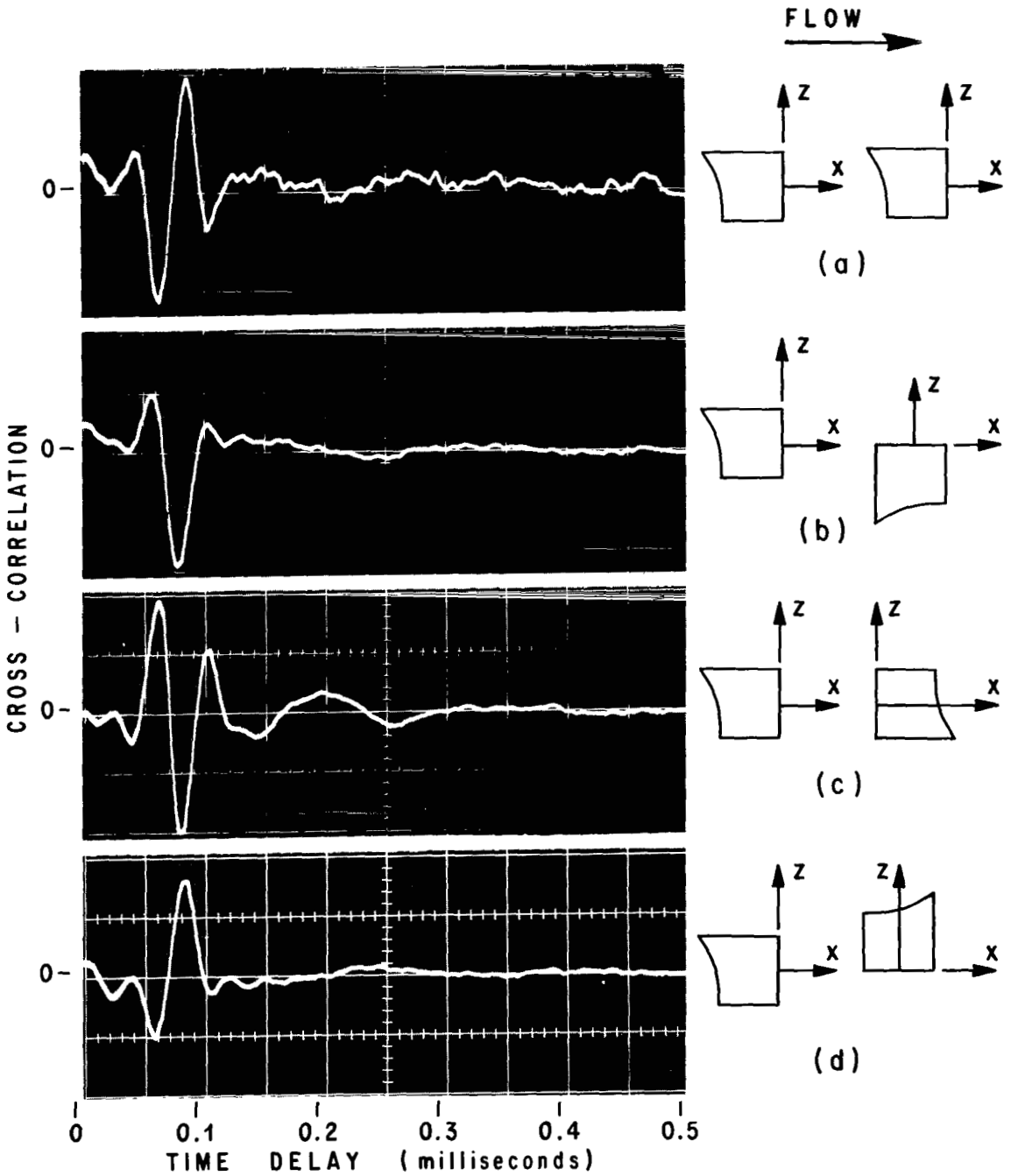

Figure 11. Cross-correlograms computed for four knife-edge arrangements as shown.

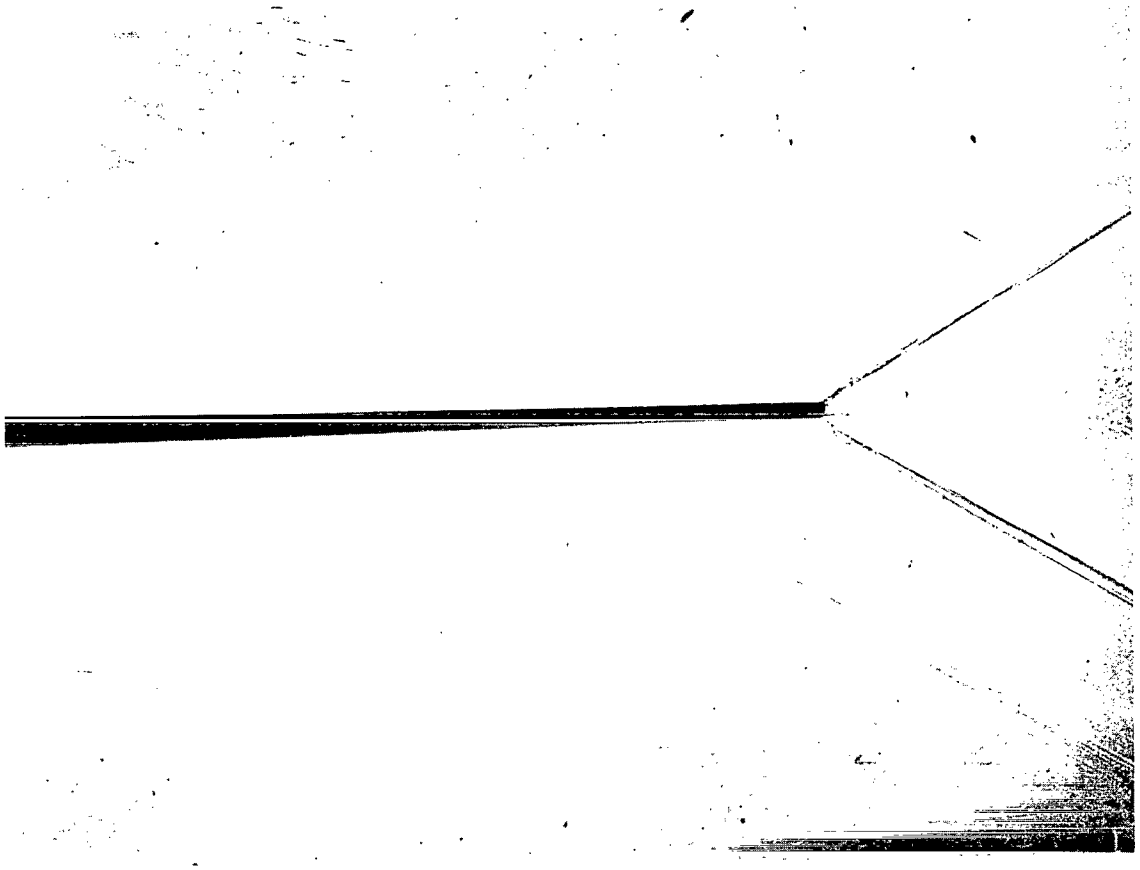

Figure 12. Shadowgraph of flow field generated by the thin plate model.

REFERENCES

1. Funk, B. H., and Cikanek, H. A., Jr.: Optical Probing of Supersonic Aerodynamic Turbulence with Statistical Correlation. Phase I: Feasibility. NASA TM X-53850, June 9, 1969.

2. Cambel, A. B., and Jennings, B. H.: Gas Dynamics. McGraw-Hill Book Co., Inc., New York, 1958.

3. Bendat, J. S., and Pierson, A. G.: Measurement and Analysis of Random Data. John Wiley, New York, 1966.

4. Fisher, M. J., and Krause, F. R.: The Cross Beam Correlation Technique. J. Fluid Mech., vol. 28, part 4, 1967, pp. 705-717.

NASA-Langley, 1970 —— 1 M164

"The aeronautical and space activities of the United States shall be conducted so as to contribute . . . to the expansion of human knowledge of phenomena in the atmosphere and space. The Administration shall provide for the widest practicable and appropriate dissemination of information concerning its activities and the results thereof."

—NATIONAL AERONAUTICS AND SPACE ACT OF 1958

NASA SCIENTIFIC AND TECHNICAL PUBLICATIONS

TECHNICAL REPORTS: Scientific and technical information considered important, complete, and a lasting contribution to existing knowledge.

TECHNICAL NOTES: Information less broad in scope but nevertheless of importance as a contribution to existing knowledge.

TECHNICAL MEMORANDUMS: Information receiving limited distribution because of preliminary data, security classification, or other reasons.

CONTRACTOR REPORTS: Scientific and technical information generated under a NASA contract or grant and considered an important contribution to existing knowledge.

TECHNICAL TRANSLATIONS: Information published in a foreign language considered to merit NASA distribution in English.

SPECIAL PUBLICATIONS: Information derived from or of value to NASA activities. Publications include conference proceedings, monographs, data compilations, handbooks, sourcebooks, and special bibliographies.

TECHNOLOGY UTILIZATION PUBLICATIONS: Information on technology used by NASA that may be of particular interest in commercial and other non-aerospace applications. Publications include Tech Briefs, Technology Utilization Reports and Notes, and Technology Surveys.

Details on the availability of these publications may be obtained from:

SCIENTIFIC AND TECHNICAL INFORMATION DIVISION

NATIONAL AERONAUTICS AND SPACE ADMINISTRATION

Washington, D.C. 20546